JACS
JOURNAL OF THE AMERICAN CHEMICAL SOCIETY
Communication
pubs.acs.org/JACS

Valence Band Dependent Charge Transport in Bulk Molecular Electronic Devices Incorporating Highly Conjugated Multi-[(Porphinato)Metal] Oligomers

Robert C. Bruce,[†,§] Ruobing Wang,[‡,§] Jeff Rawson,[‡] Michael J. Therien,[*,‡] and Wei You[*,†]

[†]Department of Chemistry, University of North Carolina at Chapel Hill, Chapel Hill, North Carolina 27599, United States
[‡]Department of Chemistry, Duke University, Durham, North Carolina 27708, United States

Supporting Information

ABSTRACT: Molecular electronics offers the potential to control device functions through the fundamental electronic properties of individual molecules, but realization of such possibilities is typically frustrated when such specialized molecules are integrated into a larger area device. Here we utilize highly conjugated (porphinato)-metal-based oligomers ($\mathbf{PM_n}$ structures) as molecular wire components of nanotransfer printed (nTP) molecular junctions; electrical characterization of these "bulk" nTP devices highlights device resistances that depend on $\mathbf{PM_n}$ wire length. Device resistance measurements, determined as a function of $\mathbf{PM_n}$ molecular length, were utilized to evaluate the magnitude of a phenomenological β corresponding to the resistance decay parameter across the barrier; these data show that the magnitude of this β value is modulated via porphyrin macrocycle central metal atom substitution [$\beta(\mathbf{PZn_n}$; 0.065 Å^{-1}) < $\beta(\mathbf{PCu_n}$; 0.132 Å^{-1}) < $\beta(\mathbf{PNi_n}$; 0.176 Å^{-1})]. Cyclic voltammetric data, and ultraviolet photoelectron spectroscopic studies carried out at gold surfaces, demonstrate that these nTP device resistances track with the valence band energy levels of the $\mathbf{PM_n}$ wire, which were modulated via porphyrin macrocycle central metal atom substitution. This study demonstrates the ability to fabricate "bulk" and scalable electronic devices in which function derives from the electronic properties of discrete single molecules, and underscores how a critical device function—wire resistance—may be straightforwardly engineered by $\mathbf{PM_n}$ molecular composition.

Designing electronic components at the single molecule level promises extremely high density devices, offering an alternative solution to circumvent limitations that will soon face silicon-based technologies.[1] The promise and power of molecular electronics (ME) come in large part from the tunable properties that have been demonstrated and realized through a host of single molecule (or few molecule) structure−property measurements.[2] For example, modulating the redox states[3] or conjugation properties of molecules[4] has been shown to alter measured single molecule conductance values. Likewise, specialized inorganic complexes, such as valence tautomers and spin crossover complexes,[5] highlight approaches to regulate molecular conductance and spin states and suggest strategies to develop organic spin valve devices.[6]

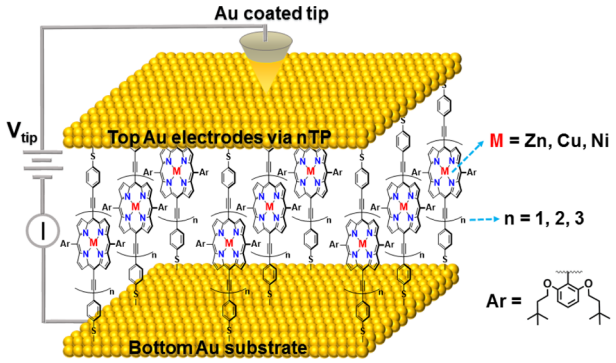

Figure 1. Device schematic highlighting α,ω-di[(4′-thiophenyl)-ethynyl]-terminated *meso*-to-*meso* ethyne-bridged (porphinato)metal-(II) oligomers (**dithiol-$\mathbf{PM_n}$** wires; M = Zn(II), Cu(II), or Ni(II); n = 1−3), assembled on a bottom gold substrate, and wired into an electrical device with a top gold electrode attached via nTP. A gold-coated AFM tip is used to electrically address the nTP devices.

One class of conjugated molecular wires that displays exceptional optoelectronic properties and shows promise for implementation in ME is *meso*-to-*meso* ethyne-bridged (porphinato)zinc(II) oligomers ($\mathbf{PZn_n}$, Figure 1).[7] Steady-state and time-resolved electronic absorption spectroscopy establish that $\mathbf{PZn_n}$ oligomers evince lowest excited singlet states that are globally delocalized.[7b,c] Variable-temperature solution-phase X-band electron spin resonance spectroscopic studies of *p*-doped $\mathbf{PZn_n}$ showed that $[\mathbf{PZn_n}]^+$ structures feature the longest hole polaron delocalization lengths yet measured for a π-conjugated material in solution (∼7.5 nm).[7d] Break junction single molecule conductance measurements of thiol-terminated $\mathbf{PZn_n}$ have demonstrated a distance-dependent junction resistance that followed exponential behavior ($R = R_0 e^{\beta L}$, where R_0 is the contact resistance, β is the phenomenological resistance decay parameter across the barrier, and L the molecular length). A phenomenological β value of 0.034 Å^{-1} determined for $\mathbf{PZn_n}$, among the lowest yet determined for thiol-terminated single molecules, establishes the potential for these π-conjugated structures as molecular wires at electrode interfaces. Congruent with these exceptional properties, these structures have been utilized in a

Received: October 14, 2015
Published: February 1, 2016

ACS Publications © 2016 American Chemical Society

DOI: 10.1021/jacs.5b10772
J. Am. Chem. Soc. 2016, 138, 2078−2081

number of nanoscale devices that take advantage of their remarkable optoelectronic properties.[8]

One key difficulty in ME is observing molecule-based properties in practical device settings. ME devices have been designed and tested through methods such as scanning tunneling microscope (STM) break junctions,[9] conducting atomic force microscopy (c-AFM),[10] or EGaIn electrodes,[11] but these techniques are presently analytic in nature and not usable in practical settings. To overcome this hurdle, a range of techniques have been developed to provide permanent device settings.[12] In particular, soft lithographic transfer of metal contacts enables working electrodes to be transferred onto organic materials without damaging the active layer.[13] These techniques have been shown to work with basic organic monolayers, such as alkanedithiols, but beyond this, device output becomes inconsistent with that determined for analogous single molecule measurements, due to factors that include extensive molecular aggregation.[14] Thus, it is clear that developing practical "bulk" devices that possess functions that derive from properties of organized collections of single molecules is nontrivial.

Here, we incorporate terminally functionalized *meso*-to-*meso* ethyne-bridged (porphinato)metal(II) oligomers (**PM$_n$** structures) into nanotransfer printed (nTP) devices, which integrate thousands of these molecules into a "bulk" ME junction (Figure 1). We then electrically characterize "bulk" nTP devices that exploit α,ω-di[(4′-thiophenyl)ethynyl]-terminated-**PM$_n$** (**dithiol-PM$_n$**) molecules, and determine how measured device resistances depend on **PM$_n$** wire length and the nature of the metal center. We further compare this dependence to earlier work that evaluated single molecule resistances via molecular break junction measurements, to investigate how the "bulk" device setting impacts distance-dependent resistance measurements.

The design, synthesis, and characterization of S-acetyl-protected α,ω-di[(4′-thiophenyl)ethynyl]-terminated (porphinato)metal compounds (**PM$_n$(SAc)$_2$**) are described in the Supporting Information. Monolayers of **dithiol-PM$_n$** were prepared on gold substrates from 0.1 M THF (M = Zn, Ni) or CH_2Cl_2 (M = Cu) solutions *via in situ* deprotection using ammonium hydroxide. Note that these **dithiol-PM$_n$** structures are based on 10,20-bis(2′,6′-bis(3,3-dimethyl-1-butyloxy)-phenyl)porphyrin building blocks; the steric interaction between the porphyrin β-hydrogen atoms and the 10- and 20-phenyl ring ortho-alkoxy substituents is substantial, severely restricting the extent of aryl ring vibrational motion as well as the range of accessible torsional angles between the phenyl and porphyrin least-squares planes at ambient temperature.[15] The phenyl 2′,6′-bis(3,3-dimethyl-1-butyloxy) substituents thus lie approximately orthogonal to the porphyrin plane, preventing **dithiol-PM$_n$** aggregation and providing self-assembled monolayers that are not densely packed on Au surfaces. Investigation of optimized, as-prepared SAMs of **dithiol-PM$_n$** on Au by X-ray photoelectron spectroscopy (XPS) indicates a significant fraction of **dithiol-PM$_n$** species lying flat on the surface, evidenced by the relative bound and unbound S 2p spectra thiol signal intensities (Supporting Information). Electrical measurements (*vide infra*) ultimately probe the dominant population of **dithiol-PM$_n$** species standing off the surface.

Figure 1 outlines the integration of **dithiol-PM$_n$** wires into a device setting. nTP was used to print 200 nm diameter gold contacts onto the **dithiol-PM$_n$** monolayers; a gold coated AFM tip allowed for electrical characterization of the nTP devices. The advantage of nTP is that it prints a large number of top contacts across each monolayer, allowing for measurement of many devices on the same substrate. Figure 2 presents a summary of

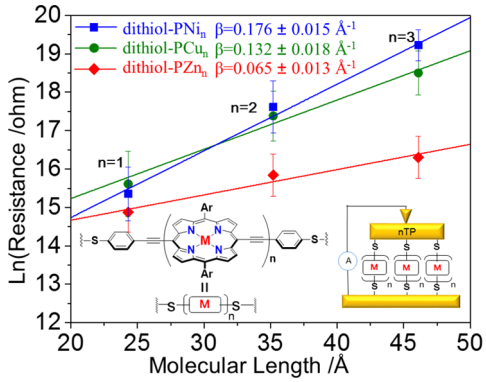

Figure 2. Natural logarithmic plots of measured resistance versus molecular length for **dithiol-PM$_n$** structures determined in nTP devices as a function of molecular wire length and the nature of the porphyrin macrocycle central metal ion. Red, M = Zn(II); green, M = Cu(II); blue, M = Ni(II). Error bars represent one standard deviation.

electrical data measured across numerous **PM$_n$** devices; each data point corresponds to the average of the values obtained on several gold-on-silicon substrates (Supporting Information). For each **dithiol-PM$_n$** composition, we evaluate the resistance decay parameter across the barrier, β, from fitting an exponential to experimental resistance values determined in these nTP devices as a function of molecular length. While the magnitude of β is affected by multiple parameters,[13] here we use it to characterize a phenomenological distance dependence of experimentally determined nTP molecular device resistances, and probe the impact of the nature of **dithiol-PM$_n$** metal center on measured resistance in an nTP device setting (Figure 2).

The first point that should be highlighted is the nearly identical phenomenological β value (β = 0.065 Å^{-1}, Figure 2, red line) obtained from the nTP junctions constructed with **dithiol-PZn$_n$** wires relative to previously reported break junction single molecule conductance measurements that examined these identical molecules (β = 0.034 Å^{-1}).[7e] This finding is noteworthy for two reasons. First, the similar resistance attenuation values offer direct evidence that nTP is a viable and reliable method for designing "bulk" ME junctions with these specialized porphyrin wires. Second, it contrasts data acquired for previously characterized large area molecular junctions that exploit densely packed phenylenedithiols, which exhibit diminished β values relative to that determined in single molecule measurements.[14] Such effects presumably trace their genesis to electronic states and charge transport pathways made possible in molecular aggregates that are not relevant to the conductance properties of isolated single molecules. For **dithiol-PM$_n$**, intermolecular interactions that lead to these additional charge transport pathways in densely packed monolayers are sterically precluded (*vide supra*); as a result, the phenomenological β value obtained from the nTP junction data for **dithiol-PZn$_n$** species mirrors that evaluated from single molecule break junction experiments.

With **dithiol-PZn$_n$**-based nTP devices validating that single molecule resistance attenuation properties are preserved in a practical device setting, analogous **dithiol-PCu$_n$** and **dithiol-PNi$_n$** structures were incorporated into nTP "bulk" ME junctions. Similar electrical measurements and β value determinations were performed (Figure 2). The increases in the magnitude of the phenomenological β for **dithiol-PCu$_n$** and **dithiol-PNi$_n$**

DOI: 10.1021/jacs.5b10772
J. Am. Chem. Soc. 2016, 138, 2078−2081

molecular wires relative to **dithiol-PZn$_n$** reflect a gradual transition of the charge transport process from a regime where a mix of tunneling, hopping, and resonant transport mechanisms operate (**dithiol-PZn$_n$**),[7e,16] to those where more classic tunneling behavior is exhibited (**dithiol-PCu$_n$**, **dithiol-PNi$_n$**). While previous work established a dependence of single molecule resistances for monomeric (porphinato)metal complexes upon the nature of the central metal ion (M = Ni, Co, Cu),[17] this work demonstrates for the first time a macrocycle central metal ion dependence of the experimentally determined β value for porphyrin oligomer-based wires in an ME device. These findings, discovered in a "bulk" device setting, not only highlight the intrinsic capability to modify the charge transport properties of **dithiol-PM$_n$** wires via metal center variation but underscore the suitability of these molecules for more practical and scalable device applications.

To understand the impact of the nature of the macrocycle central metal ion on the molecular length-dependent resistances measured for these **PM$_n$** wires in nTP device settings, cyclic voltammetric (CV) experiments were utilized to determine the $E_{1/2}{}^{0/+}$ values for the S-acetyl-protected **PM$_n$(SAc)$_2$** molecules in solution (Figure 3). Because charge transport through the

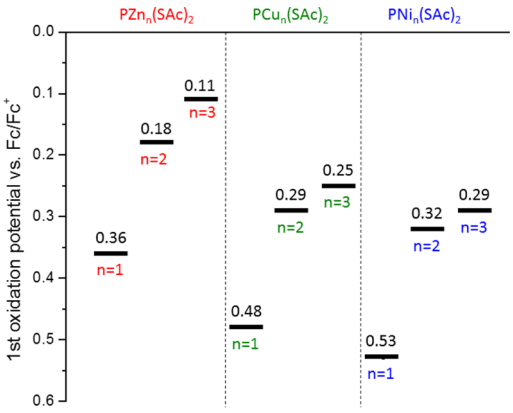

Figure 3. Potentiometrically determined HOMO energy levels for S-acetyl-protected **dithiol-PM$_n$** structures (**PM$_n$(SAc)$_2$**) from cyclic voltammetric data. These redox potentials are shown relative to the ferrocene/ferrocenium (Fc/Fc^+) redox couple, which was used as an internal standard in these experiments. Experimental conditions: solvent = CH_2Cl_2, [chromophore] = 2 mM, [NBu_4PF_6] = 0.1 M, scan rate = 100 mV/s, T = 25 °C.

porphyrins is hole mediated,[14,8a,16a,18] these potentiometrically determined HOMO energy levels provide qualitative insight into the barriers associated with the **dithiol-PM$_n$** junctions. As indicated by Figure 3, lowering the HOMO energy level leads to a larger barrier height for hole transport, congruent with the Figure 2 data that show β(**PZn$_n$**) < β(**PCu$_n$**) < β(**PNi$_n$**).

While the Figure 3 data highlight **PM$_n$(SAc)$_2$** solution $E_{1/2}{}^{0/+}$ values, it is known that surface interactions can shift energy levels and effective barrier heights.[19] Due to the inability to spectroscopically address **dithiol-PM$_n$** molecules in a fully finished device, we probed **dithiol-PM$_n$** HOMO levels relative to vacuum in the closest configuration possible to that of the final device, as monolayers on gold, via ultraviolet photoelectron spectroscopic (UPS) experiments. Figure 4 displays the UPS data from the Fermi level region acquired for each **PM$_n$** monomer. Note that the estimated barrier heights determined from these experiments ($E_F - E_{HOMO}$, Table 1) track with the macrocycle central-metal-ion-dependent $E_{1/2}{}^{0/+}$ value shifts chronicled in

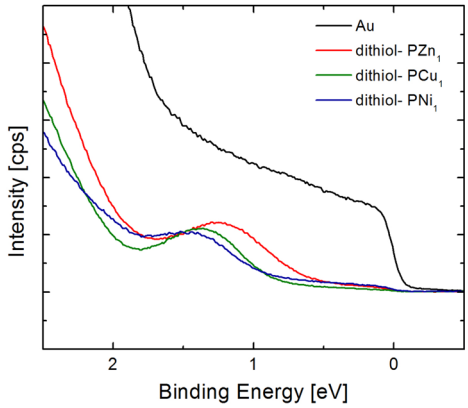

Figure 4. Fermi level region UPS data for **dithiol-PM$_1$** (red = Zn(II), green = Cu(II), blue = Ni(II)), compared against a bare gold substrate (black line).

Table 1. UPS Data Acquired for dithiol-PM$_1$ on Au Substrates

Molecule	Cutoff Energy (eV)	ϕ_{SAM}[a] (eV)	$\Delta\phi_{SAM}$ (eV)	$E_F - E_{HOMO}$[b] (eV)
Au	16.06	5.14	–	–
dithiol-PZn$_1$	16.94	4.26	0.88	0.42
dithiol-PCu$_1$	17.01	4.19	0.95	0.58
dithiol-PNi$_1$	17.02	4.18	0.96	0.65

[a]Calculated using the equation KE = $h\nu$ − BE − ϕ_{SAM}, where KE is kinetic energy, BE is the binding energy, and $h\nu$ is the ionization source energy (21.2 eV, He(I); see Supporting Information). [b]Obtained from the BE corresponding to the first peak after the Fermi level of Au (E_F defined at BE = 0 eV).

Figure 3. Previous studies show that the charge transport barrier determined from spectroscopic $E_F - E_{HOMO}$ offsets may be lower than those evaluated from electrically measured barrier heights.[19] Congruently, earlier computational studies indicate that transport barriers as large as ~0.5 eV produced mixed tunneling and resonant transport channels due to energy level broadening of the molecular states at the electrode surface.[20] Similarly, flickering or transient resonant mechanisms have been proposed to describe charge transfer in these strongly coupled **PM$_n$** oligomers,[21] when the barrier height is of the magnitude accessed in these experiments.

These UPS data also demonstrate that the electronic structure of the **dithiol-PM$_n$** wire does not impact appreciably the nature of the Au−monolayer interface. Table 1 tabulates the results and also highlights that the work function of the gold surface, $\Delta\phi_{SAM}$, is identical within the experimental error (0.1 eV) characteristic of these measurements, indicating that local electrostatic effects of all the **dithiol-PM$_1$** monolayers are similar and that these Au−molecule interfaces are indistinguishable. Note in this regard that the Table 1 $E_F - E_{HOMO}$ values, which provide an estimate of the barrier height for hole transport, are larger in magnitude that this 0.1 eV error, congruent with the picture that the modulations in the magnitude of β that are observed in these **dithiol-PM$_n$** nTP devices derive from the electronic structure of the molecular wire, which is modulated by the nature of the macrocycle central metal ion, and not from a disparate character of the molecule−electrode interface. While UPS is unable to probe the Au interface of **dithiol-PM$_2$** and **dithiol-PM$_3$** monolayers due to their extended molecular lengths and the low electron escape depth of the technique,[19b] XPS data (Supporting Information) indicate that **dithiol-PM$_n$** interfaces are identical irrespective of molecular

DOI: 10.1021/jacs.5b10772
J. Am. Chem. Soc. 2016, 138, 2078−2081

length. Therefore, as with the **dithiol-PM$_1$** monolayers, nTP device electronic properties will be dictated by the nature of the metal center and map the electrochemical data of Figure 3, and not governed by interfacial interactions.

In conclusion, terminally functionalized *meso*-to-*meso* ethyne-bridged (porphinato)metal(II) oligomers (**dithiol-PM$_n$** structures) have been incorporated as monolayers into "bulk" molecular electronic devices by nTP. Conductive-AFM characterization of these devices demonstrates that device resistances depend on **PM$_n$** wire length; this dependence parallels that evaluated previously in single molecule break junction measurements,[7e] underscoring that nTP is a viable and reliable method for designing "bulk" molecular electronic junctions with these specialized porphyrin wires. Cyclic voltammetric data, and UPS studies carried out at gold surfaces, indicate that these nTP device resistances track with the valence band energy level of the **PM$_n$** wire. These findings highlight the ability to fabricate "bulk" and *scalable* molecular electronic devices by nTP in which function derives from the electronic properties of discrete single molecules, and underscore how a critical device function—wire resistance—may be straightforwardly engineered in **PM$_n$** compositions. This work further suggests opportunities for incorporating metal ions with unpaired electrons into **PM$_n$** wires and the evolution of nTP devices for spintronics,[6b] as well as **PM$_n$**-based nTP devices where metal ion axial ligand binding events manipulate junction electrical output.[3,8a,22]

■ ASSOCIATED CONTENT

Supporting Information

The Supporting Information is available free of charge on the ACS Publications website at DOI: 10.1021/jacs.5b10772.

Detailed synthetic and substrate preparation procedures, XPS and UPS data, nTP printing process procedures and device details, description of the statistical evaluation of charge transport data acquired in nTP devices (PDF)

■ AUTHOR INFORMATION

Corresponding Authors

*michael.therien@duke.edu

*wyou@unc.edu

Author Contributions

§R.C.B. and R.W. contributed equally to this work.

Notes

The authors declare no competing financial interest.

■ ACKNOWLEDGMENTS

R.C.B. and W.Y. acknowledge support from National Science Foundation through Grants CHE-1058626 and CHE-1412286. R.W. and M.J.T. acknowledge the Division of Chemical Sciences, Geosciences, and Biosciences, Office of Basic Energy Sciences, of the U.S. Department of Energy through Grant DE-SC0001517, for support.

■ REFERENCES

(1) Markov, I. L. *Nature* **2014**, *512*, 147.

(2) Aradhya, S. V.; Venkataraman, L. *Nat. Nanotechnol.* **2013**, *8*, 399.

(3) Baghernejad, M.; Zhao, X.; Ørnsø, K. B.; Füeg, M.; Moreno-García, P.; Rudnev, A. V.; Kaliginedi, V.; Vesztergom, S.; Huang, C.; Hong, W.; Broekmann, P.; Wandlowski, T.; Thygesen, K. S.; Bryce, M. R. *J. Am. Chem. Soc.* **2014**, *136*, 17922.

(4) Jia, C.; Wang, J.; Yao, C.; Cao, Y.; Zhong, Y.; Liu, Z.; Liu, Z.; Guo, X. *Angew. Chem., Int. Ed.* **2013**, *52*, 8666.

(5) (a) Schmidt, R. D.; Shultz, D. A.; Martin, J. D.; Boyle, P. D. *J. Am. Chem. Soc.* **2010**, *132*, 6261. (b) Pronschinske, A.; Bruce, R. C.; Lewis, G.; Chen, Y.; Calzolari, A.; Buongiorno-Nardelli, M.; Shultz, D. A.; You, W.; Dougherty, D. B. *Chem. Commun.* **2013**, *49*, 10446.

(6) (a) Zhang, X.; Mizukami, S.; Kubota, T.; Ma, Q.; Oogane, M.; Naganuma, H.; Ando, Y.; Miyazaki, T. *Nat. Commun.* **2013**, *4*, 1392. (b) Cho, W. J.; Cho, Y.; Min, S. K.; Kim, W. Y.; Kim, K. S. *J. Am. Chem. Soc.* **2011**, *133*, 9364.

(7) (a) Lin, V. S.-Y.; DiMagno, S. G.; Therien, M. J. *Science* **1994**, *264*, 1105. (b) Susumu, K.; Therien, M. J. *J. Am. Chem. Soc.* **2002**, *124*, 8550. (c) Duncan, T. V.; Susumu, K.; Sinks, L. E.; Therien, M. J. *J. Am. Chem. Soc.* **2006**, *128*, 9000. (d) Susumu, K.; Frail, P. R.; Angiolillo, P. J.; Therien, M. J. *J. Am. Chem. Soc.* **2006**, *128*, 8380. (e) Li, Z.; Park, T.-H.; Rawson, J.; Therien, M. J.; Borguet, E. *Nano Lett.* **2012**, *12*, 2722. (f) Rawson, J.; Angiolillo, P. J.; Frail, P. R.; Goodenough, I.; Therien, M. J. *J. Phys. Chem. B* **2015**, *119*, 7681. (g) Rawson, J.; Angiolillo, P. J.; Therien, M. J. *Proc. Natl. Acad. Sci. U. S. A.* **2015**, *112*, 13779.

(8) (a) Banerjee, P.; Conklin, D.; Nanayakkara, S.; Park, T.-H.; Therien, M. J.; Bonnell, D. A. *ACS Nano* **2010**, *4*, 1019. (b) Conklin, D.; Park, T.-H.; Nanayakkara, S.; Therien, M. J.; Bonnell, D. A. *Adv. Funct. Mater.* **2011**, *21*, 4712.

(9) Xu, B.; Tao, N. J. *Science* **2003**, *301*, 1221.

(10) Kim, B.; Beebe, J. M.; Jun, Y.; Zhu, X.-Y.; Frisbie, C. D. *J. Am. Chem. Soc.* **2006**, *128*, 4970.

(11) Baghbanzadeh, M.; Simeone, F. C.; Bowers, C. M.; Liao, K.-C.; Thuo, M.; Baghbanzadeh, M.; Miller, M. S.; Carmichael, T. B.; Whitesides, G. M. *J. Am. Chem. Soc.* **2014**, *136*, 16919.

(12) (a) Seo, S.; Min, M.; Lee, J.; Lee, T.; Choi, S.-Y.; Lee, H. *Angew. Chem., Int. Ed.* **2012**, *51*, 108. (b) Akkerman, H. B.; Blom, P. W. M.; de Leeuw, D. M.; de Boer, B. *Nature* **2006**, *441*, 69.

(13) Niskala, J. R.; Rice, W. C.; Bruce, R. C.; Merkel, T. J.; Tsui, F.; You, W. *J. Am. Chem. Soc.* **2012**, *134*, 12072.

(14) (a) Wold, D. J.; Haag, R.; Rampi, M. A.; Frisbie, C. D. *J. Phys. Chem. B* **2002**, *106*, 2813. (b) Kronemeijer, A. J.; Huisman, E. H.; Akkerman, H. B.; Goossens, A. M.; Katsouras, I.; van Hal, P. A.; Geuns, T. C. T.; van der Molen, S. J.; Blom, P. W. M.; de Leeuw, D. M. *Appl. Phys. Lett.* **2010**, *97*, 173302.

(15) (a) Uyeda, H. T.; Zhao, Y.; Wostyn, K.; Asselberghs, I.; Clays, K.; Persoons, A.; Therien, M. J. *J. Am. Chem. Soc.* **2002**, *124*, 13806. (b) Nikiforov, M. P.; Zerweck, U.; Milde, P.; Loppacher, C.; Park, T.-H.; Uyeda, H. T.; Therien, M. J.; Eng, L.; Bonnell, D. *Nano Lett.* **2008**, *8*, 110.

(16) (a) Sedghi, G.; García-Suárez, V. M.; Esdaile, L. J.; Anderson, H. L.; Lambert, C. J.; Martin, S.; Bethell, D.; Higgins, S. J.; Elliott, M.; Bennett, N.; Macdonald, J. E.; Nichols, R. J. *Nat. Nanotechnol.* **2011**, *6*, 517. (b) Sedghi, G.; Esdaile, L. J.; Anderson, H. L.; Martin, S.; Bethell, D.; Higgins, S. J.; Nichols, R. J. *Adv. Mater.* **2012**, *24*, 653. (c) Sedghi, G.; Sawada, K.; Esdaile, L. J.; Hoffmann, M.; Anderson, H. L.; Bethell, D.; Haiss, W.; Higgins, S. J.; Nichols, R. J. *J. Am. Chem. Soc.* **2008**, *130*, 8582.

(17) Liu, Z.-F.; Wei, S.; Yoon, H.; Adak, O.; Ponce, I.; Jiang, Y.; Jang, W.-D.; Campos, L. M.; Venkataraman, L.; Neaton, J. B. *Nano Lett.* **2014**, *14*, 5365.

(18) (a) Li, Z.; Smeu, M.; Park, T.-H.; Rawson, J.; Xing, Y.; Therien, M. J.; Ratner, M. A.; Borguet, E. *Nano Lett.* **2014**, *14*, 5493. (b) Conklin, D.; Nanayakkara, S.; Park, T.-H.; Lagadec, M. F.; Stecher, J. T.; Therien, M. J.; Bonnell, D. A. *Nano Lett.* **2012**, *12*, 2414.

(19) (a) Kim, B.; Choi, S. H.; Zhu, X.-Y.; Frisbie, C. D. *J. Am. Chem. Soc.* **2011**, *133*, 19864. (b) D'Andrade, B. W.; Datta, S.; Forrest, S. R.; Djurovich, P.; Polikarpov, E.; Thompson, M. E. *Org. Electron.* **2005**, *6*, 11.

(20) Xing, Y.; Park, T.-H.; Venkatramani, R.; Keinan, S.; Beratan, D. N.; Therien, M. J.; Borguet, E. *J. Am. Chem. Soc.* **2010**, *132*, 7946.

(21) Zhang, Y.; Liu, C.; Balaeff, A.; Skourtis, S. S.; Beratan, D. N. *Proc. Natl. Acad. Sci. U. S. A.* **2014**, *111*, 10049.

(22) Flechtner, K.; Kretschmann, A.; Steinrück, H.-P.; Gottfried, J. M. *J. Am. Chem. Soc.* **2007**, *129*, 12110.

DOI: 10.1021/jacs.5b10772
J. Am. Chem. Soc. 2016, 138, 2078−2081